Check for updates

Identifying the deep groundwater recharge processes in an intermountain basin using the hydrogeochemical and water isotope characteristics

Bijay Man Shakya, Takashi Nakamura, Suresh Das Shrestha and Kei Nishida

ABSTRACT

The hydrogeochemical and stable isotopes of water (δD and δ^{18}O) were combined to investigate the deep groundwater recharge processes in the geologically complex intermountain basin (Kathmandu Valley). Results of the stable isotopic composition of the deep groundwater compared with global and local meteoric water lines and d-excess showed the deep groundwater as a meteoric water origin which is insignificantly affected by evaporation. The analysis suggests the deep groundwater was recharged during high rainfall periods (wet season). Additionally, the control of seasonal variation was absent in the deep groundwater and in the spring water samples. The large range of isotopic composition distribution was due to the altitude affect, whereas variations are from the various geological settings of the infiltration encountered during the recharge processes. The tri-linear diagram showed Na-K-HCO_3 and Ca-Mg-HCO_3 as the two major water types. The distribution of water types in this intermountain basin was found to be unique compared to other basins. Ionic concentration of the samples was found to be higher in the central part than in the periphery due to the ion exchange processes. This study determines the spatial distribution of various recharge processes that depends upon the environment during rainfall and the geological settings.

Key words | chemical composition, groundwater recharge, intermountain basin, Kathmandu Valley, stable isotopes of water

Bijay Man Shakya
Integrated Graduate School of Medicine, Engineering and Agricultural Sciences,
University of Yamanashi,
Yamanashi 400-8511,
Japan

Takashi Nakamura (corresponding author)
Kei Nishida
Interdisciplinary Research Centre for River Basin Environment,
University of Yamanashi,
Yamanashi 400-8511,
Japan
E-mail: *tnakamura@yamanashi.ac.jp*

Suresh Das Shrestha
Central Department of Geology,
Tribhuvan University,
Kirtipur, Kathmandu,
Nepal

INTRODUCTION

Groundwater recharge in basins surrounded by mountains on all sides is affected by the spatial distribution pattern of precipitation, the topography, and the basin system (Duffy & Al Hassan 1988). The dependency of the growing population in these basins is sensitive to the stresses related to the groundwater recharge. Understanding groundwater recharge processes in a closed intermountain basin provides the basis for establishing the sustainability and vulnerability of groundwater. Moreover, it minimizes groundwater extraction consequences such as groundwater depletion and contamination transport (Keesari *et al.* 2017).

Some studies identified the recharge processes of groundwater basins on the basis of long-term observations (Chiogna *et al.* 2014; Yang *et al.* 2018), flow model (Ella *et al.* 2002; Andreu *et al.* 2011), chemical composition (Al-Khatib & Al-Najar 2011; Blanchette *et al.* 2013). However, areas with limited hydrometric data face challenges in the estimation of recharge processes using the approaches as explained above. In such cases, combining the analysis of stable isotopic compositions of water and its hydrochemical parameters have been a useful tracer approach in identifying the hydrological processes (Clark & Fritz 1997; Vanderzalm

doi: 10.2166/nh.2019.164

Downloaded from http://iwaponline.com/hr/article-pdf/50/5/1216/610887/nh0501216.pdf
by guest

et al. 2011; Liu & Yamanaka 2012). The stable isotopic ratios of water (δD and δ^{18}O) have been useful in identifying the environmental processes during groundwater recharge as well as identifying the mixing of various groundwater sources (Weyhenmeyer et al. 2002; Li et al. 2005; Nakamura et al. 2016), while hydrochemical information can be used to support the isotopic information (Liu & Yamanaka 2012). Stable isotopes of water and hydrochemical analysis have been successful in delineating mountain block recharge (Yuan et al. 2018) and identifying the vertical interaction in deep groundwater (Onodera et al. 1995; Zhang et al. 2016). Nonetheless, identification of the deep groundwater recharge environment in the complex intermountain basin that are also overexploited by artificial pumping is ambiguous. Thus, detailed spatial investigation is required for developing a framework for further research and approaches such as modelling in the data scarce basins.

Kathmandu Valley, Nepal, is one of the largest tectonically uplifted closed intermountain basins in the Himalayan region (Sakai 2001). The watershed is surrounded by rugged mountains with the Bagmati river as a single outlet for the surface water. The Kathmandu valley is home for a population of 2.5 million (CBS 2011). As reported by the sole potable water supply company Kathmandu Upatyaka Khanepani Limited (KUKL), the water demand in this valley reaches 377 million liters per day (MLD) and they manage to supply 120 MLD of water in the wet season and 73 MLD during the dry season. The water demand deficit is covered by traditional stone spouts and shallow groundwater wells. Meanwhile, shallow wells are found to be contaminated by unmanaged septic tanks and sewer lines (Warner et al. 2008; Nakamura et al. 2014; Shrestha et al. 2014). As a result, deep groundwater is extensively extracted as a basic drinking water supply source. According to KUKL (2017), the deep groundwater contributes 15.4% of the total water supply. Though the extraction scenario increased, the deep groundwater recharge processes are not yet clearly understood. The deep groundwater recharge occurs from the north and south-eastern parts of the Kathmandu Valley (JICA 1990; Pandey et al. 2010), whereas the recharge in the central part is restricted by a ~200 m thick lacustrine deposit (JICA 1990; Gurung et al. 2006). Furthermore, the central part of the valley is stated as stagnant, and the development of deep tube wells for artificial groundwater extractions are recommended to be restricted due to the recharge conditions (JICA 1990). Lately, the extension of groundwater extraction has resulted in the depletion and drawdown of the groundwater level in the Kathmandu Valley (Udmale et al. 2016; Thapa et al. 2017). Previously, numerous studies have been carried out to characterize the problems such as depletion of deep groundwater in the Kathmandu Valley (Pandey et al. 2012; Gautam & Prajapati 2014) and understanding the hydrogeochemical environment (Gurung et al. 2006; Chapagain et al. 2009b). Earlier studies regarding the recharge processes in the studied area were related to the shallow groundwater (Nakamura et al. 2012; Malla et al. 2015). The recharge processes of the deep groundwater along with its spatial distribution in the intermountain basin is not well understood. However, a closer look is essential for identifying the local influence on recharge processes of the watershed.

The objective of this study is to identify the deep groundwater recharge environment in an intermountain basin and spatial distribution of the recharge processes. This study also attempts to identify any vertical or lateral recharge in the deep groundwater situated in the densely populated area. The study uses the combination of stable isotopic compositions of water and hydrochemical analysis of the groundwater for the first time in the Kathmandu Valley in order to investigate the environment of recharge processes.

MATERIALS AND METHODS

Study area

The Kathmandu Valley basin is located between latitudes N 27°32′34″ and N 27°49′11″ and longitudes E 85°11′10″ and E 85°31′10″. The amphitheatre-shaped valley stretches in the direction of 30 km E-W and 25 km N-S and covers an area of 664 km^2 with elevations ranging from 1,212 to 2,722 m above sea level (Figure 1) (Thapa et al. 2017). The valley is surrounded by several mountains with elevations greater than 2,000 m (JICA 1990). The mean annual rainfall on the valley floor is 1,500 mm, while the surrounding hills receive 1,800 mm (Thapa et al. 2017); 80% of the total rainfall occurs during June to mid-September (monsoon),

Downloaded from http://iwaponline.com/hr/article-pdf/50/5/1216/610887/nh0501216.pdf
by guest

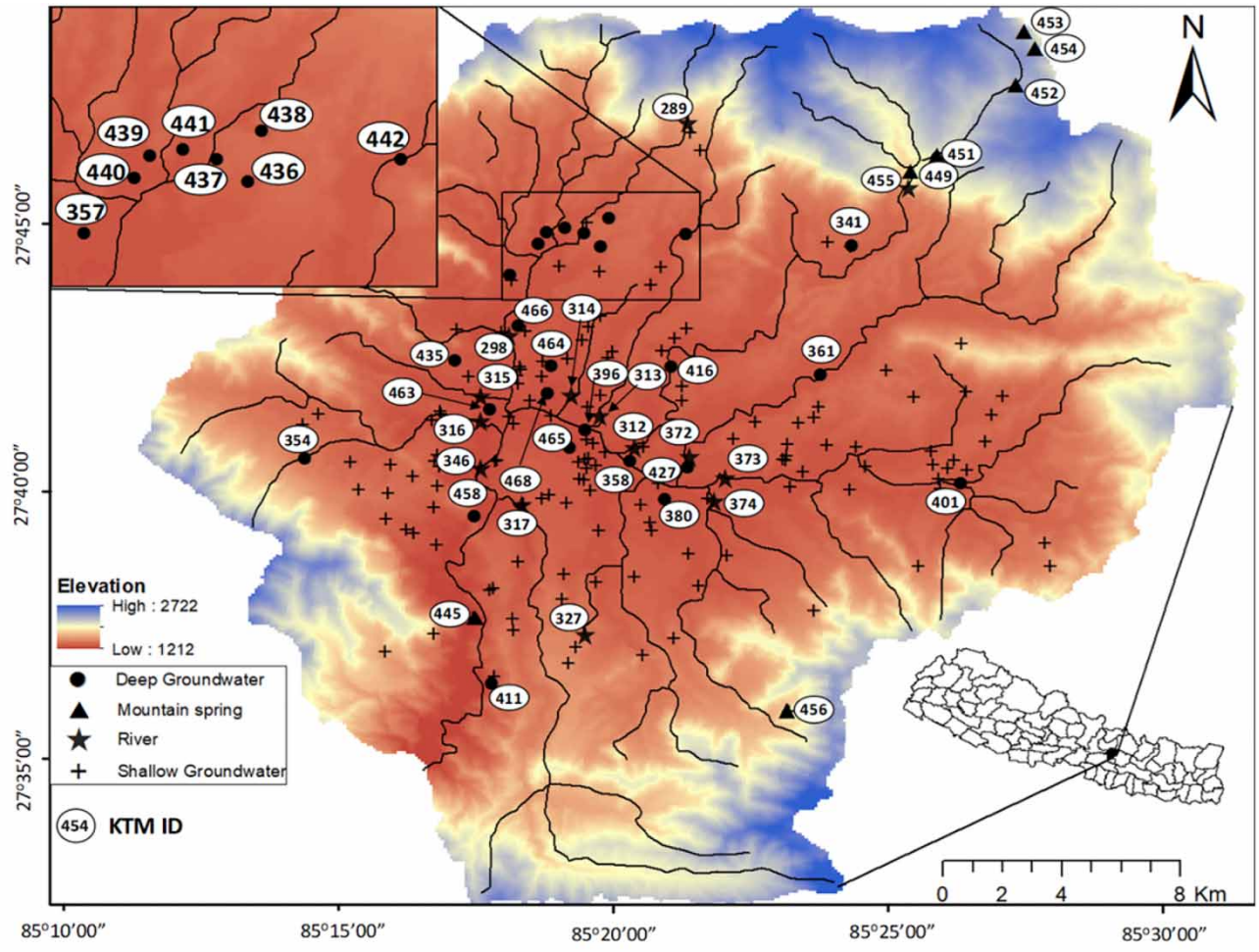

Figure 1 | Sampling location of deep groundwater, spring, shallow groundwater and river water in Kathmandu Valley.

considered as the wet season, while the dry season occurs during November to mid-February with little rainfall (Pandey *et al.* 2010).

Geology and hydrogeology

The valley basin rests on the Kathmandu Nappe (Sakai 2001) which are intensely folded, faulted and fractured (Shrestha 2012). Four hundred million years (Ma) old igneous and metamorphic (Sheopuri Gneiss) rocks are found to the north and east, while sedimentary basement rocks are found to the south and west (Dhital 2015) (Figure 2).

The valley is comprised of Plio-Pleistocene sediment infill of fluvial, fluvio-lacustrine, and deltaic sediments, mainly unconsolidated to semi-consolidated sand, gravel, peat, silt, clay, and carbonaceous black shale brought from the surrounding hills (Sakai 2001; Dhital 2015). In general, the central portion of the valley is dominated by thick black clay (Kalimati Clay) overlain by sand and silty clay. The northern part is covered by sand and gravel deposit, whereas the southern parts consist of interbedded clay, silt and sand beds. The N-S schematic cross-section of the Kathmandu Valley is shown in Figure 3.

The valley aquifer is divided into shallow and deep systems, where the deep aquifer depth is 60 m below the ground surface (Gurung *et al.* 2006). A thick aquitard of ~200 m clay separates the deep groundwater from the shallow groundwater and is distributed mostly toward the central part of the valley with the thickness gradually decreasing towards the valley margins (JICA 1990;

Downloaded from http://iwaponline.com/hr/article-pdf/50/5/1216/610887/nh0501216.pdf
by guest

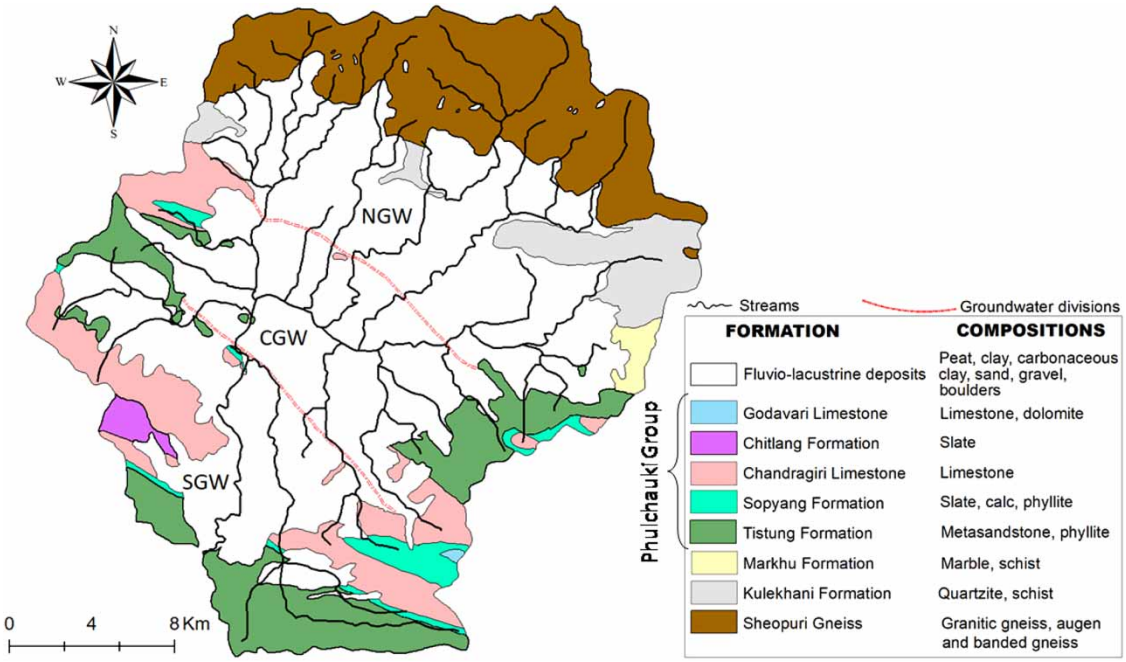

Figure 2 | Bedrock formations and respective lithological composition of Kathmandu Valley (modified from DMG/BGR/DOI 1998). Solid line represents streams. Dashed line shows groundwater district division by JICA (1990) separating North Groundwater district (NGW), Central Groundwater district (CGW) and Southern Groundwater district (SGW).

Metcalf & Eddy 2000). A piezometric surface map and a groundwater flow path of the study area show that the deep groundwater flows towards the center of the valley, mostly governed by the slope direction (Shrestha *et al.* 1996; Cresswell *et al.* 2001). JICA (1990) delineated three groundwater zones in the Kathmandu Valley floor: the northern groundwater district (NGW), the central groundwater district (CGW) and the southern groundwater district (SGW) (Figure 2); in addition, NGW was identified as the major deep groundwater recharge area in the valley.

Sampling

A field survey was carried out from August to September 2016. Overall, 25 deep groundwater samples were collected from deep tube wells with 75–285 m depth located in the densely populated area. Fourteen river water samples were collected from the elevation ranging from 1,270 to 1,500 m (Figure 1). In addition, natural spring water samples were collected from five different locations at elevations ranging from 1,450 to 2,087 m in the northern mountain during the wet season. Meanwhile, two spring water samples

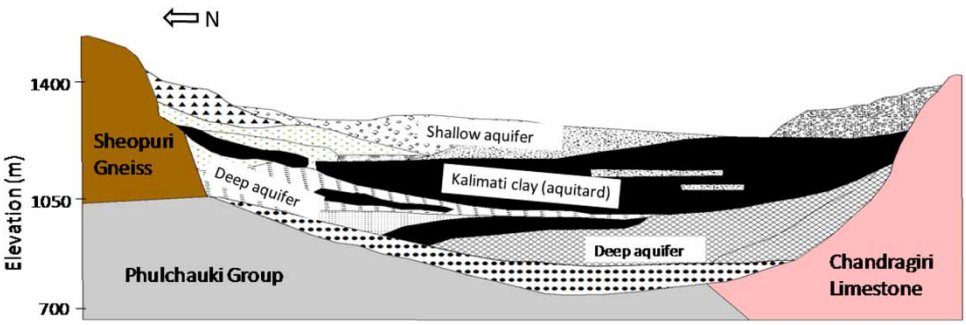

Figure 3 | North–south schematic cross-section of Kathmandu Valley showing the fluvio-lacustrine deposits (modified after Gurung *et al.* 2007).

Downloaded from http://iwaponline.com/hr/article-pdf/50/5/1216/610887/nh0501216.pdf
by guest

were collected during both dry and wet seasons from the southern mountains located at an elevation of 1,475 and 1,516 m (Figure 1). Based on the field survey, the spring water samples collected from the northern mountain originated from the cracks in granitic gneiss whereas those in the southern mountains are from the fractures in limestone. Similarly, 130 shallow groundwater samples were collected from private and community wells in the valley (Figure 1).

The water samples were analyzed for their isotopic and chemical compositions at the Interdisciplinary Centre for River Basin Environment, University of Yamanashi (ICRE-UY). The hydrogen and oxygen stable isotopic compositions of the water samples were determined using cavity ring-down spectroscopy (L1102-i, Picarro, Santa Clara, CA, USA). The stable hydrogen and oxygen isotope ratios are expressed as δD and δ^{18}O, respectively, relative to the Vienna Standard Mean Ocean Water (VSMOW). The analytical errors were 0.5‰ for δD and 0.1‰ for δ^{18}O.

The isotopic ratios (δD and δ^{18}O) were reported relative to the VSMOW standard (Craig 1961), given by:

$$\delta\mathrm{D} \text{ or } \delta^{18}\mathrm{O} = \frac{(R_{sample} - R_{V-SMOW})}{R_{V-SMOW}} \times 1000\ (‰) \qquad (1)$$

where R indicates the isotopic ratio of D and ^{1}H or ^{18}O and ^{16}O.

The cation and anion concentrations were measured using an ion chromatograph (ICS-1100, Dionex, USA) with an analytical error of 5%, and the bicarbonate concentrations were measured using the titration method (pH 4.8) with 0.1 N H_2SO_4.

RESULTS

Chemical composition

The major cations and anions in the sampled water sources are shown in Table 1.

The variation of Cl^- concentrations was largest in shallow groundwater (1.6–217 mg/L), whereas the lowest concentration was in mountain springs (0.4–0.5 mg/L) (Figure 4). The Cl^- concentrations of the river water ranged from 0.5 to 65.9 mg/L. In the Bagmati river, the Cl^- concentration varied with altitude, upstream (>1,450 m), midstream (1,280 m), and downstream (<1,280 m) (Figure 5). Land use in the Kathmandu Valley is related to altitude and most human activities are concentrated in the central part and at lower altitudes (<1,450 m). The presence of halite rocks in this area are never reported by researchers, the Cl^- concentration occurred geochemically or due to anthropogenic activities. Overall, the chloride concentration of deep groundwater shows low variability, ranging from 0.5 to 14.9 mg/L. However, a high Cl^- concentration of 51.1 mg/L was detected in sample KTM 463 located in the central part of the valley (Figure 1).

The water quality data plotted in the trilinear diagram suggests bicarbonate-dominated deep groundwater of Ca-Mg-HCO_3 and Na-K-HCO_3 chemical composition types (Figure 6(a)). Most of the deep groundwater collected from the central (KTM 380, 396, 401, 427, 463, and 465) and southern (KTM 354, 357, 411, 435 and 458) parts of the valley were found to be of Ca-Mg-HCO_3 type (Figure 1). Na-K-HCO_3 type deep groundwater samples are distributed in the northern part of the valley (KTM 361, 416, 442, and 437). Other samples from the central part (KTM 358, 464 and 468) and northwest part (KTM 341, 436, 438, 439, 440, and 441) show Na^+ dominance (Figure 6(a)). Northern mountain spring water is classified as Na-K-HCO_3 type. Similarly, river water samples were of two types: Ca-Mg-HCO_3 type flowing from the southern part and Na-K-HCO_3 type flowing from the northern part of the valley (Figure 6(b)).

Isotopic compositions

Groundwater samples

Plots of δ^{18}O versus δD (Figure 7(a) and 7(b)) show that all deep and shallow groundwater samples follow a similar trend to the global meteoric water line (GMWL) (Craig 1961) and the local meteoric water line (LMWL) (Gajurel *et al.* 2006), showing strong meteoric origin. Also, most of the deep groundwater samples were placed below the meteoric water lines. The fractionation of isotopes during evaporation causes enrichment of stable isotopes of water during rainfall and also makes a trend line of slope less

Downloaded from http://iwaponline.com/hr/article-pdf/50/5/1216/610887/nh0501216.pdf
by guest

Table 1 | Sampled location data, hydrochemical and isotopic values from the studied area

Source	Sample ID	North	East	Na^+ (mg/l)	K^+ (mg/l)	Ca^{2+} (mg/l)	Mg^{2+} (mg/l)	Cl^- (mg/l)	SO_4^{2-} (mg/l)	HCO_3^- (mg/l)	Water isotope (‰) $\delta^{18}O$	δD
Spring	KTM 445 (wet)	27.627	85.291	–	–	–	–	–	–	–	−9	−61
	KTM 445 (dry)										−9.4	−62
	KTM 449	27.766	85.424	6.8	0.8	3	0.8	0.6	nd.	40.3	−8.3	−56
	KTM 451	27.773	85.43	3.8	0.1	0.3	nd.	0.5	nd.	13.4	−8.8	−60
	KTM 452	27.795	85.456	2.7	0.5	0.7	0.2	0.4	0.4	15.3	−9	−61
	KTM 453	27.809	85.458	2.2	0.1	0.4	0.2	0.5	nd.	7.9	−9.3	−63
	KTM 454	27.806	85.464	1	0.1	0.2	nd.	0.5	nd.	7.6	−9.2	−62
	KTM 456 (wet)	27.598	85.387	–	–	–	–	–	–	–	−9	−61
	KTM 456 (dry)										−9.4	−62
Deep groundwater	KTM 341	27.743	85.405	12.3	1.3	7.7	2.9	1.9	0.8	97.6	−8.7	−62
	KTM 354	27.677	85.24	5.2	1.6	14.5	5.6	6.6	4.2	152.5	−8.5	−57
	KTM 357	27.734	85.302	1.8	0.6	21.3	6.4	1.9	17.1	201.3	−8.2	−56
	KTM 358	27.747	85.355	59.9	8.1	30.3	11.1	1.9	0.3	366	−7.6	−52
	KTM 361	27.676	85.338	26.4	3	12.8	5.5	8.8	7.4	183	−9.1	−64
	KTM 380	27.664	85.349	22.2	7.6	35.5	13.1	1.7	0.3	469.7	−8.9	−65
	KTM 396	27.703	85.396	61	12	68.8	14	2.1	nd.	579.5	−7.6	−53
	KTM 401	27.686	85.325	17.8	4.2	23.8	3.7	0.6	nd.	256.2	−9.7	−71
	KTM 411	27.669	85.439	1.9	0.9	16.3	7.8	1.8	8.8	146.4	−8.9	−62
	KTM 416	27.607	85.296	54	4.5	22.8	6.6	6.5	nd.	433.1	−8	−55
	KTM 427	27.705	85.351	49.9	11.5	42.4	13.4	1.4	nd.	701.5	−7.9	−53
	KTM 435	27.707	85.285	25.1	6.9	49.4	5.7	3	nd.	524.6	−8.6	−62
	KTM 436	27.743	85.33	17	1.5	11.2	3.8	2.9	4.2	106.8	−9.5	−68
	KTM 437	27.674	85.356	17	1.3	8.6	3.4	0.5	nd.	109.8	−9.4	−68
	KTM 438	27.747	85.313	15.4	1.2	10	3.1	0.5	0.7	100.7	−9.6	−69
	KTM 439	27.752	85.332	16.2	1.4	10.6	3.5	0.5	nd.	115.9	−9.5	−68
	KTM 440	27.744	85.311	16.6	1.4	9.9	3.4	0.6	nd.	119	−9.4	−67
	KTM 441	27.749	85.319	16.5	1.2	8.6	3.5	0.6	nd.	97.6	−9.6	−68
	KTM 442	27.747	85.324	2.8	0.5	1.8	0.4	0.6	0.6	97.6	−8.9	−59
	KTM 458	27.743	85.405	26.9	3.9	34.7	7.4	14.9	19.5	334.6	−8.6	−62
	KTM 463	27.692	85.296	68	8.5	63.9	41.2	51.1	0.7	877.5	−7.1	−49
	KTM 464	27.705	85.315	17.5	2.2	11.3	3.9	1	1.2	123.5	−8.4	−57
	KTM 465	27.68	85.32	40	17.2	59.6	18.5	2.4	nd.	754.6	−8.3	−59
	KTM 466	27.718	85.305	53.7	5.4	24.2	10.3	3.3	nd.	542.9	−8.5	−60
	KTM 468	27.697	85.313	40	6.8	33.9	8.2	1.2	nd.	597.8	−7	−47
SGW ($n = 130$)	Mean	–	–	44.7	24.9	39.8	14.5	64	43.4	196.9	−7.8	−54
	Median	–	–	40.9	9.3	31.8	13.1	54	34.5	170.8	−7.8	−54
	Min.	–	–	0.6	0.3	3.6	0.6	1.6	0.5	36.3	−9.4	−69
	Max.	–	–	176.6	162	120.3	52.9	217	294	542.9	−5.5	−37
River	KTM 289	27.782	85.356	3.2	0.7	2.8	0.2	1.6	0.9	30.5	−8.9	−58
	KTM 298	27.715	85.301	26	7.6	19.1	3.4	24.9	14.7	158.6	−8.9	−63
	KTM 312	27.683	85.339	11.6	3.1	5.4	1.2	8.9	4.3	63.4	−8.7	−59
	KTM 313	27.69	85.328	45.2	12.9	20.2	4.8	42.9	19.8	195.2	−8.3	−58
	KTM 314	27.697	85.319	57.8	22.9	39.5	7.4	59.9	28.4	39	−8.4	−60
	KTM 315	27.696	85.293	64.9	15.6	37.4	9.9	66	27.6	330.2	−8	−56
	KTM 316	27.686	85.293	52.6	13.8	33.6	11.8	61	19.4	334.3	−7.7	−55
	KTM 317	27.662	85.306	6.9	1.6	22.7	4.6	6	3.9	329.3	−8.9	−63
	KTM 327	27.62	85.333	7	2.1	13.2	2.6	6.3	4.9	91.5	−9.6	−71
	KTM 346	27.674	85.293	26.3	7.1	16.9	4.6	24.2	11.7	189.1	−8.6	−60
	KTM 372	27.675	85.355	6.6	1.4	5.9	1	4.4	2.8	250	−7.8	−57
	KTM 373	27.673	85.365	35.4	10.7	27.8	6.7	36.2	17.2	300	−7.3	−54
	KTM 374	27.664	85.363	7.1	1.2	16.4	4.4	7.5	5.4	300	−8.3	−63
	KTM 455	27.763	85.424	2.6	0.5	1.5	0.3	0.5	0.4	30	−8.9	−60

SGW, shallow groundwater; nd., non-detected; dry and wet, seasons of data collection.

Downloaded from http://iwaponline.com/hr/article-pdf/50/5/1216/610887/nh0501216.pdf
by guest

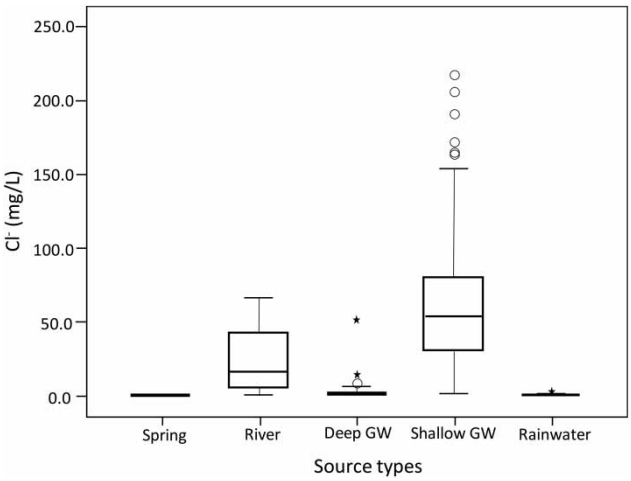

Figure 4 | Box plot comparing chloride (Cl^-) concentration obtained from the various sources. Circles represent outliers within the 1.5-interquartile range and stars indicate extreme outliers within the 3-interquartile ranges (GW = groundwater).

than 8 (Craig 1961; Clark & Fritz 1997; Yin *et al.* 2011). However, no such clear trend line was observed in the study area, suggesting no strong evaporation effect during the deep groundwater recharge. A dual isotope index, deuterium excess (d-excess or d), which is the function of $\delta^{18}O$ and δD ($d = \delta D - 8 * \delta^{18}O$), reflects the source and evolution of rainfall during vapor transport (Bershaw 2018). Referring to Gajurel *et al.* (2006) the d-excess of the local rainfall in the study area during the wet season ranged from 5 to 16‰ (average: 9‰), while it ranged from 11 to 25‰ (average: 17‰) during the dry season. The d-excess of the deep groundwater from the study area ranged between 6 and 12‰ (average: 9‰). The similarity between the deep groundwater and local rainfall shows a profound recharge from monsoon rainfall during the wet season that is less affected by evaporation for isotopic fractionation.

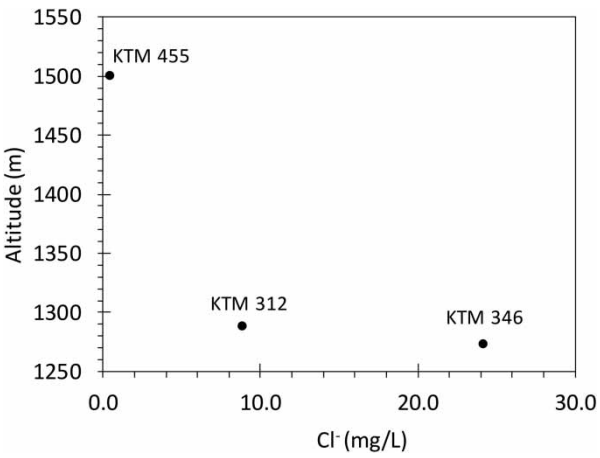

Figure 5 | Determining the extent of Cl^- source on the surface water using the Bagmati River data, running from the least populated area upstream to the densely populated area.

The δD and $\delta^{18}O$ of deep groundwater show wide ranges from −71 to −47‰ and from −9.7 to −7.6‰, respectively. Spatially, the deep groundwater in the central part of the study area has heavier δD values ranging from −65 to −47‰ and $\delta^{18}O$ values ranging from −9.6 to −7.0‰ (Figure 8). Although lying at the north, the δD and $\delta^{18}O$ of deep groundwater lying at the northwest part are comparatively lighter ranging from −69 to −67‰ and from −9.6 to −9.4‰, respectively (Figure 8). They are thus discussed separately to other parts of the valley. The δD and $\delta^{18}O$ in shallow groundwater range from −65 to −37‰ (median: −54‰) and from −9.4 to −5.5‰ (median: −7.8‰) (Table 1). Deep groundwater, except for that in the NW part of the valley, exhibits similar isotopic composition to shallow groundwater and river water.

Spring and river water

The δD and $\delta^{18}O$ values of the spring water collected from the northern mountain range from −63 to −56‰ and from −9.3 to −8.3‰, respectively. The water isotopic values vary according to the altitude (Figure 9). The stable isotopic values of spring samples collected from the southern mountain ranged from −60 to −62‰ in the dry season and −60 to −61‰ in the wet season for δD, whereas $\delta^{18}O$ in both seasons was −9‰. This result indicates no seasonal variation in the spring water samples. Similarly, the δD and $\delta^{18}O$ values of the river water samples range from −70 to −54‰ (average: −59‰) and from −7.3 to −9.6‰ (average: −8.4‰) (Table 1). Comparing the $\delta^{18}O$ and δD values in river waters, they were lower in the samples collected from the base of the mountains and were higher in lowland tributaries.

Altitude effect

To evaluate the altitude effect of rainfall, it is necessary to examine the long-term and spatially distributed rainfall

Downloaded from http://iwaponline.com/hr/article-pdf/50/5/1216/610887/nh0501216.pdf
by guest

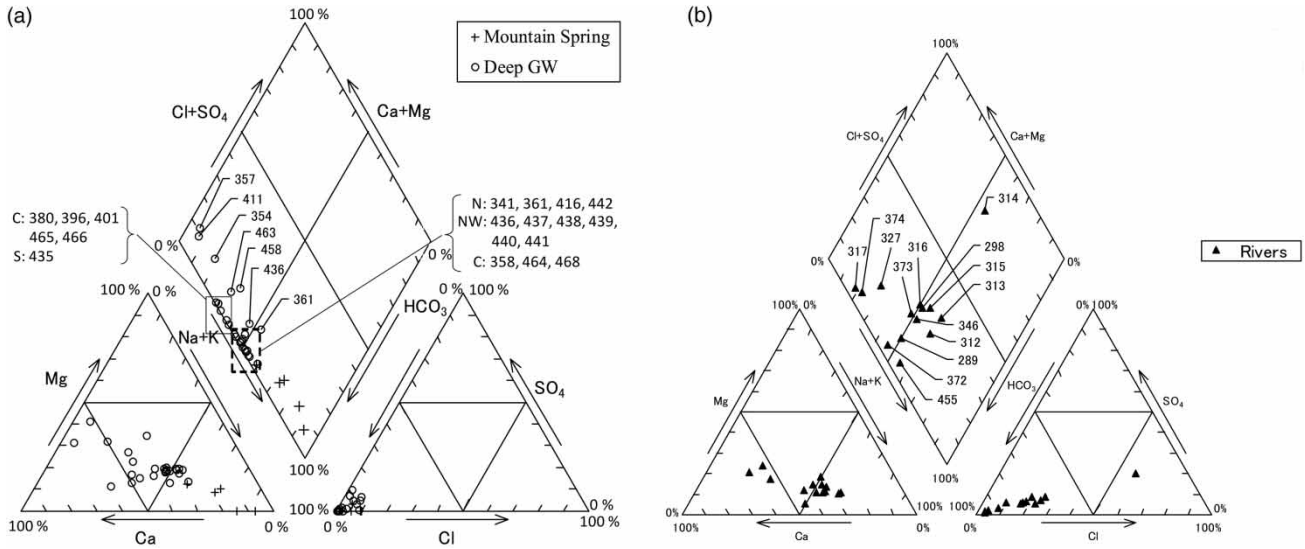

Figure 6 | Trilinear diagrams showing chemical composition type of (a) deep groundwater and mountain spring samples and (b) river water (*N* = north, NW = northwest, C = central and S = south).

records (Weyhenmeyer *et al.* 2002). The existing high-altitude spring data are appropriate for calculating the isotopic altitude effect since they are directly related to rainfall and are least affected by evaporation during recent rainfall (Gibrilla *et al.* 2017). Lighter water isotopic values in the study area are recorded in the mountainous springs (Figure 9). The water isotopic values decrease with increasing elevation from 1,450 to 2,087 m with a lapse rate of −1 and −0.15‰ per 100 m of increased elevation for δD and δ^{18}O, respectively. The lapse rate of the δD and δ^{18}O values, being −1.9 and −0.22‰ per 100 m respectively, are found to be similar to the spring water samples reported at Mt. Jamachwok at the western part of the Kathmandu Valley (Nakamura *et al.* 2012) and the lapse rate of δ^{18}O measured from multiyear precipitation data was −0.17‰ per 100 m from the Kathmandu Valley (Wen *et al.* 2011). Nevertheless, the distribution of water isotopic value and lapse rate confirms that the isotopic values of springs are linearly related to elevation, reflecting the local altitude effect in spring water. These water isotopic values can be used to estimate the recharge altitude of the spring and groundwater (Equations (2) and (3)). However, estimation of recharge origin will be difficult to use in the groundwater with evaporated infiltration, thus comparative conclusions for different water origins can be drawn using the altitude effect (Boronina *et al.* 2005). Thus, the lighter isotopic value of water in this study is inferred as recharge from higher altitude and the heavier isotopic value as recharged from lower altitude for comparative conclusions of different water origins.

$$h(m) = -101^{*}\delta\mathrm{D} - 4268 \quad (2)$$

$$h(m) = -707^{*}\delta^{18}\mathrm{O} - 4464 \quad (3)$$

DISCUSSION

Enrichment of the stable isotopic composition due to the evaporation and deviation away from MWL is significant during lighter rainfall. Less frequently, such deviation diminishes once the air column is water saturated (Yin *et al.* 2011). Moreover, the precipitation over the mountain also contains recycled evaporation from mountain forests which also increases the amount of rainfall (Peng *et al.* 2015). The deep groundwater in the study area lying near and parallel to MWL, along with the d-excess similar to the rainfall value 9‰, shows they were recharged during the heavy rainfall events of the wet season. Similar results were also reported elsewhere in a basin in Taiwan (Peng *et al.* 2015). Additionally, d-excess of the groundwater also provides the information for the seasonal variation during

Downloaded from http://iwaponline.com/hr/article-pdf/50/5/1216/610887/nh0501216.pdf
by guest

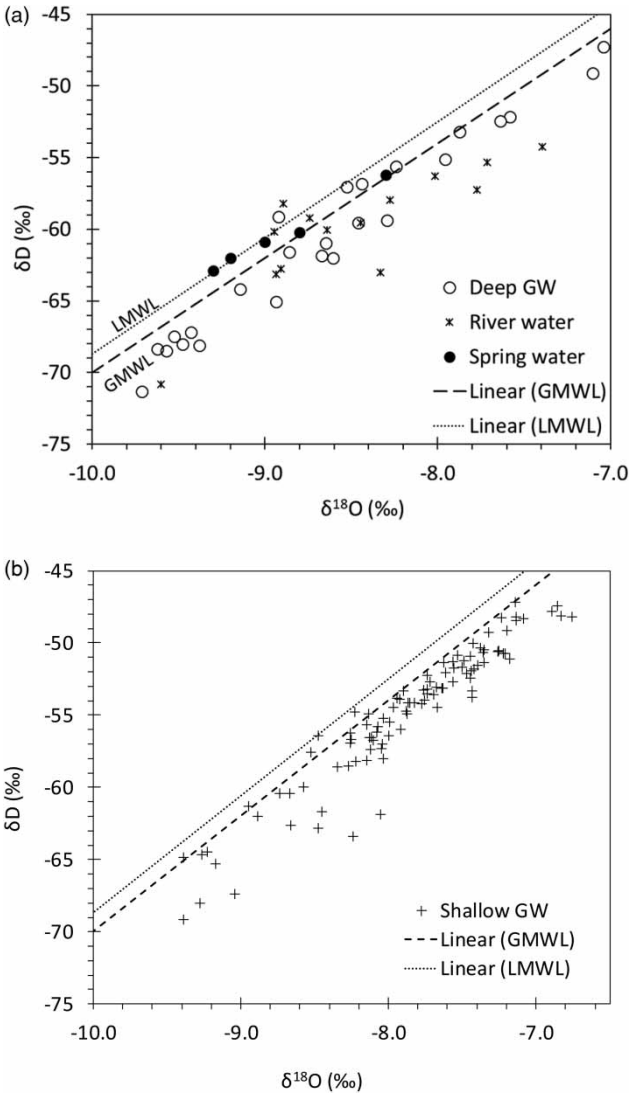

Figure 7 | δD and $\delta^{18}O$ values of (a) deep groundwater and river water samples (b) shallow groundwater samples.

the rainfall (Nakamura *et al.* 2016). On the other hand, increasing residence time (>1 year) decreases the seasonal fractionation of the groundwater isotopic compositions (Asano *et al.* 2002). The seasonal variation of d-excess during the two rainfall periods in the study area can be inferred from Gajurel *et al.* (2006). However, the deep groundwater of the Kathmandu valley shows no seasonal variation (Chapagain *et al.* 2009a). Additionally, no seasonal variation was observed between the stable isotope of water collected from the southern mountain springs. This shows that the springs are not directly affected by rainfall but the water is discharged through the crack openings after a certain period of residence time. This also infers that the residence time of groundwater and spring water are higher than the variation period. Although there is no seasonal variation, the different ranges of isotopic distribution in the deep groundwater is due to the altitude effect when recharging the groundwater during high rainfall periods.

Chemical composition type reveals the groundwater and subsurface environment in natural conditions. Ca-Mg-HCO_3 and Ca-HCO_3 types represent recent freshwater infiltration (Al-Khatib & Al-Najar 2011; Li *et al.* 2017), whereas the Na-HCO_3 type indicates ion exchange (Candela & Morell 2009; Al-Khatib & Al-Najar 2011) and relatively longer groundwater residence time (Pastorelli *et al.* 2001). As reported by JICA (1990), the northern periphery in the studied area is considered the major recharge area for deep groundwater and the central part is considered non-rechargeable stagnant (for an estimated age of 28,000 years using ^{14}C). In this context, the hydrochemical dominance of the Na-K-HCO_3 type in both spring water samples and groundwater samples in the northern parts of the valley and the dominance of the Ca-K-HCO_3 type in the central part of the study area are both unique in the Kathmandu Valley aquifer.

The difference in chemical composition type of the groundwater in the various parts of the Kathmandu Valley can be explained by considering the rock type and ion-exchange processes. The observed Na-K-HCO_3 water type in the mountain springs may be due to the dissolved Na-K salts originating from the weathered minerals of gneiss rock which dominates the geology of the northern part of the Kathmandu Valley (Figure 2). Similar to those mountain springs, the deep groundwater collected from the northern side, KTM (341 and 442) are of Na-K-HCO_3 type. The δD range in the groundwater of these samples are similar to that in the mountain spring water and river water (KTM 455 and 289) (Figure 8) showing recharge from lower altitudes, mainly mountain base recharges. The Cl^- vs δD graph (Figure 10) shows the relationship between the anthropogenic activities in river water and groundwater originating from various altitudes. Higher Cl^- concentrations in Kathmandu may be due to sewage and septic leakage (Nakamura *et al.* 2014). However, low Cl^- obtained in the northern groundwater similar to the Cl^- in spring

Downloaded from http://iwaponline.com/hr/article-pdf/50/5/1216/610887/nh0501216.pdf
by guest

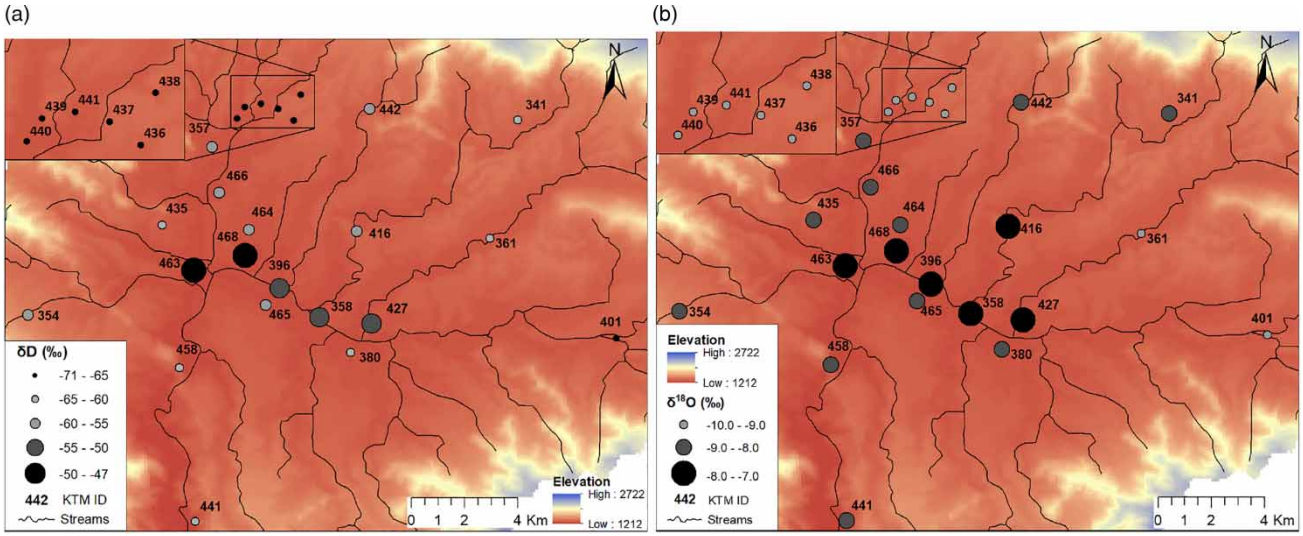

Figure 8 | Spatial distributions of (a) δD and (b) $\delta^{18}O$ values of deep groundwater samples from Kathmandu Valley.

shows no effect of anthropogenic activities on ionic increments. On the other hand, the overall ionic concentrations of northern deep groundwater are higher than the spring water samples. Referring to Pastorelli *et al.* (2001), the longtime interaction of groundwater with granitic gneiss causes enrichment of ion concentrations where Na^+ increases relatively higher than other components. Since the mountain spring water has a short residence time, the higher ionic concentrations in the northern groundwater refers to the longtime residence time of deep groundwater and are recharged from the lower altitude of northern mountains.

The decrease of water isotopic values (−69 to −67‰) observed in the NW part of the valley suggests high altitude recharge from the mountains. The lighter isotopes of water can be attributed to the precipitation from higher altitudes (Craig 1961; Clark & Fritz 1997). Apparently, no large surface-water bodies, e.g. lakes or dams, have ever been located in this area. The small range of δD value in this region implies an aquifer being fed by groundwater flowing from high altitudes through fractures or a higher capacity of localized recharge. Also, the lower Cl^- concentration (Figure 10) in the groundwater sample from the NW part of the Kathmandu valley shows recharge from those areas that are less affected by anthropogenic activities.

Water types in the central part of the valley are characterized by the dominance of Na^+ and Ca^{2+} contribution

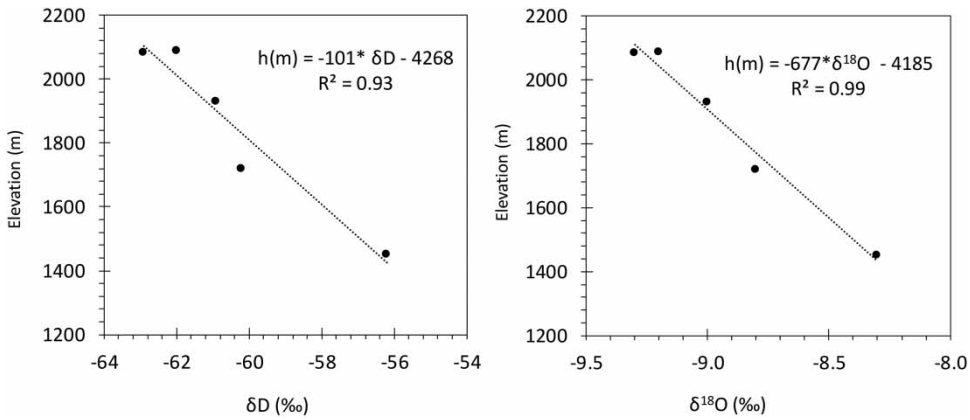

Figure 9 | Relationship between elevation, vs. δD and $\delta^{18}O$ of spring water samples collected from the Sheopuri (or Shivapuri) mountains, located in the northern part of the valley.

Downloaded from http://iwaponline.com/hr/article-pdf/50/5/1216/610887/nh0501216.pdf
by guest

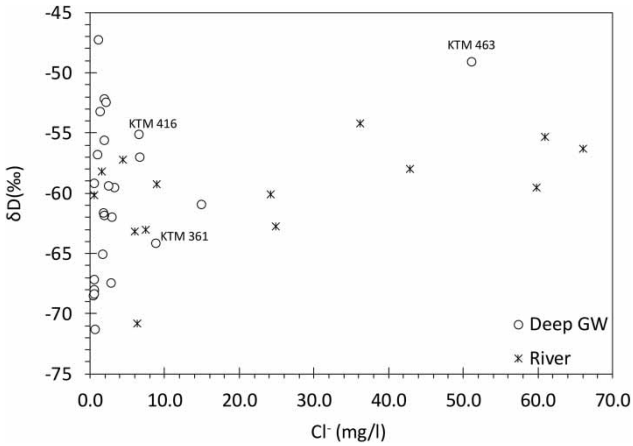

Figure 10 | Relationship between δD and Cl^- concentration.

(Figure 6(a)). Deep groundwater samples (KTM 361 and 416) show the Na-K-HCO_3 type of water, related to the groundwater from the northern side of the Kathmandu Valley. The dominance of Na^+ (Figure 6(a)) suggests that either ion exchange between the Na^+ and Ca^{2+} ions in the groundwater or recharge from the north takes place. The water isotopic signatures of these groundwater samples are heavier than those in NW groundwater (Figure 8) and are within the isotopic range of river water and shallow groundwater. Lying close to the river bank, the δD value of −64‰ in KTM 361 and −55‰ in KTM 416 is related to the river water running down from the northern mountain. Relating Cl^- with the water isotopic composition, Onodera *et al.* (2008) reported higher values of Cl^- in the deeper groundwater of Bangkok as an outcome of shallow groundwater intrusion due to over-pumping. The Cl^- concentration in the deep groundwater (ranging from 6.5 to 8.8 mg/L) suggested channel recharge from an area less affected by human activities, most likely due to the creation of a shallow pathway caused by over-pumping or tube well construction failure.

Meanwhile, the heavier water isotopic values of the deep groundwater (from −65 to −49‰) are similar to those of the shallow groundwater and river water (Table 1) with a dominance of Ca-Mg-HCO_3 type in the central part of the valley. Ca-Mg-HCO_3 suggests fresh groundwater infiltration while no evaporation effect was observed in the stable isotopes of water (Figure 7). The heavier isotopes of water in shallow groundwater in the central part of the valley was found to be recharged from lower altitudes (<1,500 m) (Nakamura *et al.* 2012). The heavier water isotope value suggests vertical recharge from low altitudes. On the other hand, the low concentration of Cl^- (Figure 10) in the central part of the valley is not affected by the vertical recharge from shallow groundwater. The dense clay deposits in the central part of the valley are protected from vertical groundwater recharge. Thus, the Ca^{2+} dominance in the groundwater from the central part may not be attributed to recent infiltration. On closer inspection, the rivers originating from the southern part of the valley (KTM 317, 327, and 374) have Ca-Mg-HCO_3 type (Figure 6(b)). The southern part of the valley consists of rock sequences composed of limestone with springs originating from fractures indicating feasibility in developing suitable underground drainage systems under weathered conditions (Shrestha 2012). The Ca^{2+} dominance in the central part of the valley suggests that the recharge at the central part of the Kathmandu Valley is possibly from the western and southern part of the Kathmandu valley dominated by Ca^{2+} terrain only from the northern and southwest parts of the valley, as reported by JICA (1990), which is dominated by Na^+ and Ca^{2+}, respectively.

Despite being protected by dense clay, the higher Cl^- value of 51.1 mg/L in KTM 463 (Figure 10) in the central part of the valley indicates the intrusion from the anthropogenic affected shallow groundwater. The single point with high Cl^- concentration suggests the intrusion of shallow surface water most likely due to construction failure of a deep tube well. On the other hand, the dominance of Na^+ proportion (KTM 464, 466, and 468) in the central part suggests a different recharge process than that of the Ca^{2+} dominated groundwater. Also, their respective isotopic values of −57, −60, and −47‰ heavier than those isotopic values recorded from the groundwater in the NW part indicates local recharge from a lower altitude. However, the low Cl^- concentration suggests that this recharge water does not originate from an anthropogenically affected area. Hydrochemically, the excess cation proportion in groundwater is balanced by Cl^- (Sheikhy Narany *et al.* 2014), and the Na^+ dominance and low Cl^- concentration in these three groundwater bodies reflect reverse ion exchange in the clay/weathered aquifer of the central part of the valley.

Downloaded from http://iwaponline.com/hr/article-pdf/50/5/1216/610887/nh0501216.pdf
by guest

CONCLUSIONS

This study utilizes hydrochemical and environmental isotopes in identifying the recharge process of the deep groundwater in an intermountain basin. Although the mountain precipitations are influenced by the evapotranspiration from the mountain forest and recycled moisture, this study revealed that the deep groundwater of the Kathmandu valley was not influenced by the evaporation effect during recharge. No seasonal isotopic variation of the spring and groundwater showed that the recharge in the deep groundwater is from the high frequency rainfall during the wet season. The spatial distribution of the isotopic composition of water shows the prevalence of altitude effect. The deep groundwater is not influenced by the direct infiltration of the rainfall and is related with the residence time after the rainfall that mostly took place in high and low altitudes. The distribution of water isotopes and hydrochemical dominance basically suggests co-occurrence of different recharge processes distributed spatially in the intermountain basin. Na-K-HCO_3 and Ca-Mg-HCO_3 chemical composition types of water distributed in the study area shows the influence of geological settings. The Na-K-HCO_3 and Ca-Mg-HCO_3 chemical composition types are due to the groundwater interaction with the gneiss and limestone bedrocks respectively. No significant vertical recharge in the deep groundwater was observed and the recharge is found primarily lateral from the mountain base or a local recharge. This study also pointed out the possibility of the deep groundwater recharge from southern parts of the valley rather than only from the northern and southeastern part of the valley which were considered as recharge zones. Thus, this study attempts to set up the boundary conditions for understanding the spatial distributions of recharge processes of deep groundwater in a geologically complex intermountain basin.

ACKNOWLEDGEMENTS

The authors would like to thank Dr Sadhana Shrestha, Niva Sthapit (University of Yamanashi) and Rajendra Budhathoki (Geologist, Beni Hydropower Project Pvt. Ltd). We also appreciate anonymous peer reviewers for their keen opinions and suggestions in preparing our manuscript. This study was financially supported by Science and Technology Research Partnership for Sustainable Development (SATREPS), funded from the Japan International Cooperation Agency (JICA) and Japan Science and Technology (JST), and by Grants-in-Aid for Scientific Research (KAKENHI).

REFERENCES

Asano, Y., Uchida, T. & Ohte, N. 2002 Residence times and flow paths of water in steep unchannelled catchments, Tanakamai, Japan. *J. Hydrol.* **261**, 173–192.

Al-Khatib, M. & Al-Najar, H. 2011 Hydro-geochemical characteristics of groundwater beneath the Gaza strip. *J. Water Resour. Prot.* **3**, 341–348.

Andreu, J. M., Alcalá, F. J., Vallejos, Á. & Pulido-Bosch, A. 2011 Recharge to mountainous carbonated aquifers in SE Spain: different approaches and new challenges. *J. Arid Environ.* **75**, 1262–1270.

Bershaw, J. 2018 Controls on deuterium excess across Asia. *Geosciences* **8**, 257.

Blanchette, D., Lefebvre, R., Nastev, M. & Cloutier, V. 2013 Groundwater quality, geochemical processes and groundwater evolution in the Chateauguay River, Quebec. *Can. Water Resour. J.* **35**, 503–526.

Boronina, A., Balderer, W., Renard, P. & Stichler, W. 2005 Study of stable isotopes in the Kouris catchment (Cyprus) for the description of the regional groundwater flow. *J. Hydrol.* **308**, 214–226.

Candela, L. & Morell, I. 2009 Basic chemical principles of groundwater. In: *Encyclopedia of Life Support Systems*. The United Nations Educational, Scientific and Cultural Organization (UNESCO), Paris, pp. 43–55. Available from: www.eolss.net/sample-chapters/C07/E2-09-03-04.pdf (accessed 16 November 2018).

Central Bureau of Statistics (CBS). 2011 *National Population and Housing Census 2011 (Population Projection 2011–2013)*. Central Bureau of Statistics, Kathmandu, Nepal.

Chapagain, S. K., Shrestha, S., Nakamura, T., Pandey, V. P. & Kazama, F. 2009a Arsenic occurrence in groundwater of Kathmandu Valley, Nepal. *Desal. Water Treat.* **4**, 248–254.

Chapagain, S. K., Pandey, V. P., Shrestha, S., Nakamura, T. & Kazama, F. 2009b Assessment of deep groundwater quality in Kathmandu Valley using multivariate statistical techniques. *Water Air Soil Pollut.* **210**, 277–288.

Chiogna, G., Santoni, E., Camin, F., Tonon, A., Majone, B., Trenti, A. & Bellin, A. 2014 Stable isotope characterization of the Vermigliana catchment. *J. Hydrol.* **509**, 295–305.

Clark, I. D. & Fritz, P. 1997 *Environmental Isotopes in Hydrogeology*. Lewis, New York, USA.

Downloaded from http://iwaponline.com/hr/article-pdf/50/5/1216/610887/nh0501216.pdf
by guest

Craig, H. 1961 Isotopic variations in meteoric waters. *Science* **133**, 1702–1703.

Cresswell, R. G., Bauld, J., Jacobson, G., Khadka, M. S., Jha, M. G., Shreshta, M. P. & Regmi, S. 2001 A first estimate of ground water ages for the deep aquifer of the Kathmandu Basin, Nepal, using the radioisotope Chlorine-36. *Ground Water* **39**, 449–457.

Dhital, M. R. 2015 *Geology of the Nepal Himalaya: Regional Perspective of the Classic Collided Orogen*. Springer, USA.

DMG/BGR/DOI 1998 *Hydrogeological Condition and Potential Barrier Sediments in the Kathmandu Valley. Technical Cooperation Project-Environmental Geology*. Final report. Department of Mines and Geology, Kathmandu, pp. 17–59, Appendix 3.

Duffy, C. J. & Al-Hassan, S. 1988 Groundwater circulation in a closed desert basin: topographic scaling and climatic forcing. *Water Resour. Res.* **24**, 1675–1688.

Ella, V. B., Melvin, S. W., Kanwar, R. S., Jones, L. C. & Horton, R. 2002 Inverse three-dimensional groundwater modeling using the finite-difference method for recharge estimation in a glacial till aquitard. *Am. Soc. Agric. Eng.* **45**, 703–7015.

Gajurel, A. P., France-Lanord, C., Huyghe, P., Guilmette, C. & Gurung, D. 2006 C and O isotope compositions of modern fresh-water mollusc shells and river waters from the Himalaya and Ganga plain. *Chem. Geol.* **233**, 156–183.

Gautam, D. & Prajapati, R. N. 2014 Drawdown and dynamics of groundwater table in Kathmandu Valley, Nepal. *Open Hydrol. J.* **8**, 17–26.

Gibrilla, A., Adomako, D., Anornu, G., Ganyaglo, S., Stigter, T., Fianko, J. R., Rai, S. & Ako, A. A. 2017 $\Delta^{18}O$ and $\delta^{2}H$ characteristics of rainwater, groundwater and springs in a mountainous region of Ghana: implication with respect to groundwater recharge and circulation. *Sustain. Water Resour. Manag.* **3**, 413–429.

Gurung, J. K., Ishiga, H., Khadka, M. S. & Shrestha, N. R. 2006 The geochemical study of fluvio-lacustrine aquifers in the Kathmandu Basin (Nepal) and the implications for the mobilization of arsenic. *Environ. Geol.* **52**, 503–517.

Gurung, J. K., Ishiga, H., Khadka, M. S. & Shrestha, N. R. 2007 *Characterization of Groundwater in the Reference of Arsenic and Nitrate Mobilization, Kathmandu Basin, Nepal*. Available from: www.semanticscholar.org/paper/Characterization-of-groundwater-in-the-reference-of-Gurung-Ishiga/0ac4a7052aa05d333398b535702b67ee8cb4ca04 (accessed 4 February 2019).

JICA 1990 *Groundwater Management Project in Kathmandu Valley*. Final Report, main report and supporting reports, November 1990. Japan International Cooperation Agency (JICA), Tokyo.

Keesari, T., Sharma, D. A., Rishi, M. S., Pant, D., Mohokar, H. V., Jaryal, A. K. & Sinha, U. K. 2017 Isotope investigation on groundwater recharge and dynamics in shallow and deep alluvial aquifers of southwest Punjab. *Appl. Radiat. Isot.* **129**, 163–170.

KUKL 2017 *Kathmandu Upatyaka Khanepani Limited: Annual Report*, 9th anniversary. KUKL, Kathmandu.

Li, X., Hou, X. & Zhang, L. 2005 Isotope hydrochemical approach to understand the mixing relationship and renewability of the groundwater systems in Taiyuan basin, China. *J. China Univ. Geosci.* **18**, 1–4.

Li, X., Ye, S., Wang, L. & Zhang, J. 2017 Tracing groundwater recharge sources beneath a reservoir on a mountain-front plain using hydrochemistry and stable isotopes. *Water Sci. Technol. Water Supply* **17**, 1447–1457.

Liu, Y. & Yamanaka, T. 2012 Tracing groundwater recharge sources in a mountain – plain transitional area using stable isotopes and hydrochemistry. *J. Hydrol.* **464–465**, 116–126.

Malla, R., Shrestha, S., Chapagain, S. K., Shakya, M. & Nakamura, T. 2015 Physico-chemical and oxygen-hydrogen isotopic assessment of Bagmati and Bishnumati rivers and the shallow groundwater along the river corridors in Kathmandu Valley, Nepal. *J. Water Resour. Prot.* **7**, 1435–1448.

Metcalf and Eddy 2000 *Urban Water Supply Reforms in the Kathmandu Valley*. Asian Development Bank (ADB), Manila (ADB TA Number 2998-NEP).

Nakamura, T., Chapagain, S. K., Pandey, V. P., Osda, K., Nishida, K., Malla, S. S. & Kazama, F. 2012 Shallow groundwater recharge altitudes in the Kathmandu Valley. In: *Kathmandu Valley Groundwater Outlook* (S. Shrestha, D. Pradhananga & V. P. Pandey, eds). Asian Institute of Technology (AIT), The Small Earth Nepal (SEN), Center of Research for Environmental Energy and Water (CREEW), International Research Center for River Basin Management (ICRE-UY), Kathmandu, pp. 39–45.

Nakamura, T., Nishida, K., Kazama, F., Osaka, K. & Chapagain, K. S. 2014 Nitrogen contamination of shallow groundwater in Kathmandu Valley, Nepal. *J. Japanese Assoc. Hydrol. Sci.* **44**, 197–206 (in Japanese with English abstract).

Nakamura, T., Nishida, K. & Kazama, F. 2016 Influence of a dual monsoon system and two sources of groundwater recharge on Kofu basin alluvial fans, Japan. *Hydrol. Res.* **48**, 1071–1087.

Onodera, S., Kitaoka, K., Hayashi, M., Shindo, S. & Kusakabe, M. 1995 Evaluation of the groundwater recharge process in a semiarid region of Tanzania, using δD and $\delta^{18}O$ Application of Tracers in Arid Zone Hydrology. In: *Proceedings of the Vienna Symposium August, 1994*, Vol. 232. The International Association of Hydrological Sciences (IAHS) Publications, Wallingford, pp. 383–391.

Onodera, S., Saito, M., Sawano, M., Hosono, T., Taniguchi, M., Shimada, J., Umezawa, Y., Lubis, R. F., Buapeng, S. & Delinom, R. 2008 Effects of intensive urbanization on the intrusion of shallow groundwater into deep groundwater: examples from Bangkok and Jakarta. *Sci. Total Environ.* **404**, 401–410. doi:10.1016/j.scitotenv.2008.08.003

Pandey, V. P., Chapagain, S. K. & Kazama, F. 2010 Evaluation of groundwater environment of Kathmandu Valley. *Environ. Earth Sci.* **60**, 1329–1342.

Downloaded from http://iwaponline.com/hr/article-pdf/50/5/1216/610887/nh0501216.pdf
by guest

Pandey, V. P., Shrestha, S. & Kazama, F. 2012 Groundwater in the Kathmandu Valley: development dynamics, consequences and prospects for sustainable management. *Eur. Water* **37**, 3–14.

Pastorelli, S., Marini, L. & Hunziker, J. 2001 Chemistry, isotope values (δD, δ^{18}o, $\delta^{34}S_{SO4}$) and termpratures of the water inflows in two Gottthard tunnels, Swiss Alps. *Appl. Geochem.* **16**, 633–649.

Peng, T. R., Chen, K. Y., Zhan, W. J., Lu, W. C. & Tong, L. T. J. 2015 Use of stable water isotopes to identify hydrological processes of meteoric water in montane catchments. *Hydrol. Process.* **29**, 4957–4967.

Sakai, H. 2001 Stratigraphic division and sedimentary facies of the Kathmandu Basin group, Central Nepal. *J. Nepal Geol. Soc.* **25**, 19–32.

Sheikhy Narany, T., Ramli, M. F., Aris, A. Z., Sulaiman, W. N. A., Juahir, H. & Fakharian, K. 2014 Identification of the hydrogeochemical processes in groundwater using classic integrated geochemical methods and geostatistical techniques, in Amol-Babol Plain, Iran. *Sci. World J.* **15**. doi:10.1155/2014/419058.

Shrestha, S. D. 2012 Geology and hydrogeology of groundwater aquifers in the Kathmandu Valley. In: *Kathmandu Valley Groundwater Outlook* (S. Shrestha, D. Pradhananga & V. P. Pandey, eds). Asian Institute of Technology (AIT), The Small Earth Nepal (SEN), Centre of Research for Environmental Energy and Water (CREEW), International Research Centre for River Basin Management (ICRE-UY), Kathmandu, pp. 21–30.

Shrestha, S. D., Karmacharya, R. & Rao, G. K. 1996 Estimation of groundwater resources in Kathmandu. *J. Groundwater Hydrol.* **38**, 29–40.

Shrestha, S., Nakamura, T., Malla, R. & Nishida, K. 2014 Seasonal variation in the microbial quality of shallow groundwater in the Kathmandu Valley, Nepal. *Water Sci. Technol. Water Supply* **14**, 390.

Thapa, B. R., Ishidaira, H., Pandey, V. P. & Shakya, N. M. 2017 A multi-model approach for analyzing water balance dynamics in Kathmandu Valley, Nepal. *J. Hydrol. Reg. Stud.* **9**, 149–162.

Udmale, P., Ishidaira, H., Thapa, B. & Shakya, N. 2016 The status of domestic water demand: supply deficit in the Kathmandu Valley, Nepal. *Water* **8**, 196.

Vanderzalm, J. L., Jeuken, B. M., Wischusen, J. D. H., Pavelic, P., Le Gal La Salle, C., Knapton, A. & Dillon, P. J. 2011 Recharge sources and hydrogeochemical evolution of groundwater in alluvial basins in arid central Australia. *J. Hydrol.* **397**, 71–82.

Warner, N. R., Levy, J., Harpp, K. & Farruggia, F. 2008 Drinking water quality in Nepal's Kathmandu Valley: a survey and assessment of selected controlling site characteristics. *Hydrogeol. J.* **16**, 321–334.

Wen, R., Tian, L. D., Weng, Y. B., Liu, Z. F. & Zhao, Z. P. 2011 The altitude effect of δ^{18}O in precipitation and river water in the Southern Himalayas. *Chin. Sci. Bull.* **57**, 1693–1698.

Weyhenmeyer, C. E., Burns, S. J., Waber, H. N., Macumber, P. G. & Matter, A. 2002 Isotope study of moisture sources, recharge areas, and groundwater flow paths within the eastern Batinah coastal plain, Sultanate of Oman. *Water Resour. Res.* **38**, 21–22.

Yang, L., Qi, Y., Zheng, C., Andrews, C. B., Yue, S., Lin, S., Li, Y., Wang, C., Xu, Y. & Li, H. 2018 A modified water-table fluctuation method to characterize regional groundwater discharge. *Water* **10**, 1–16.

Yin, L., Hou, G., Su, X., Wang, D., Dong, J., Hao, Y. & Wang, X. 2011 Isotopes (δD and δ^{18}O) in precipitation, groundwater and surface water in the Ordos Plateau, China: implications with respect to groundwater recharge and circulation. *Hydrogeol. J.* **19**, 429.

Yuan, R., Wang, S., Yang, L., Liu, J. & Wang, P. 2018 Hydrologic processes of groundwater in a small monsoon-influenced mountainous watershed. *Hydrol. Res.* **49**, 2016–2029.

Zhang, J., Tsujimura, M., Xianfang, S. & Sakakibara, K. 2016 Using stable isotopes and major ions to investigate the interaction between shallow and deep groundwater in Baiyangdian Lake Watershed, North China Plain. *Hydrol. Res. Lett.* **10**, 67–73.

First received 2 December 2018; accepted in revised form 2 June 2019. Available online 31 July 2019

Downloaded from http://iwaponline.com/hr/article-pdf/50/5/1216/610887/nh0501216.pdf
by guest